



Towards the establishment of a green and sustainable analytical methodology for hyperspectral imaging-based authentication of wholemeal bread

Miriam Medina-García^a, Esteban A. Roca-Nasser^a, Miguel A. Martínez-Domingo^{b,**},
Eva M Valero^b, Alejandra Arroyo-Cerezo^a, Luis Cuadros-Rodríguez^a, Ana M. Jiménez-
Carvelo^{a,*}

^a Department of Analytical Chemistry, Faculty of Sciences, University of Granada, Av. Fuentenueva s.n, E-18071, Granada, Spain

^b Department of Optics, Faculty of Sciences, University of Granada, Av. Fuentenueva s.n, E-18071, Granada, Spain

ARTICLE INFO

Keywords:

Wholemeal bread
Hyperspectral imaging
Data mining
Chemometrics
Food fraud

ABSTRACT

The increased interest in whole-grain products, along non unified European regulations on the composition of wholemeal bread could lead to its misleading labelling. Therefore, to ensure the safety of consumers, both health-wise and from possible fraud, a novel hyperspectral imaging-based authentication method is being proposed, given that no previous study has combined imaging techniques with authentication of wholemeal flour content. Quantification based on pixel counting by classification (QPC) utilizes multivariate analysis methods such as PLS-DA and SVM to classify pixels within a bread sample (as Wholemeal and White flour), based on their visible-near-infrared spectra, to later estimate its proportion of wholemeal flour. This is in accordance with the heterogeneous nature of bread samples, in which individual pixels belonging to both wholemeal and white flour can be accounted for, which was proved by implementing unsupervised training techniques such as hierarchical cluster analysis (HCA). Results show that the quantification model was able to successfully predict wholemeal flour content with a maximum deviation of 8 g wholemeal flour/100 g flour from the estimated value.

1. Introduction

Bread is one of the most consumed foods worldwide and is considered a basic staple (Pico, J. et al., 2016). The simplest bread recipe consists of a mixture of whole wheat flour, water, sugar, salt, and yeast, which is then subjected to fermentation and baking. However, bread recipes have become more complex, including different kinds of flours: wholemeal, refined, and flours from different cereals such as oats, rye, spelt, etc. (Edwards, W.P., 2007; Alnaeim, T. et al., 2014).

Wholemeal flours preserve all the cereal grain components: brand, germane and endosperm. These components provide carbohydrates, fiber, vitamins, minerals, and antioxidants that are beneficial for human health (Ma, S. et al., 2021; De Angelis, Minervini, Siragusa, Rizzello, & Gobetti, 2019; Yu, L. et al., 2013). These advantageous properties have boosted consumer interest in acquiring whole-grain products, including wholemeal bread, leading to increased production. Consequently, the

establishment of quality control becomes an imperative necessity to protect consumers from fraud and to ensure their safety.

Currently, there are no unified European regulations governing the composition of wholemeal bread, and each state member has its own regulations on this product. To illustrate it, the German wholemeal regulation requires this product to contain at least 90% wholemeal flour and Danish regulations require at least 30% wholemeal. Nevertheless, Spanish regulations do not set a minimum content, though the product label must indicate the percentage of wholemeal flour (Gobierno de España, 2019; Health Promotion Knowledge Gateway, 2022; Government of UK, 2022). These discrepancies make international trade and control of this product difficult, which is aggravated by the absence of an official analytical methodology for quality control. This lacking complicates the authentication of wholemeal bread and impacts public health, which makes the development of analytical methods to assess wholemeal bread both compelling and challenging.

* Corresponding author.

** Corresponding author.

E-mail addresses: martinezm@ugr.es (M.A. Martínez-Domingo), amariajc@ugr.es (A.M. Jiménez-Carvelo).

Quality analysis of bread is one of the most widely researched areas in the food industry (Nashat, S. & Abdullah, M.Z., 2016). Some studies have explored different analytical methods to determine the physical and chemical characteristics of bread such as, texture, colour, individual fatty acids and soluble sugar content, etc. (Riyanto, R.A. & Caraka, R. E., 2018; Caroch, M. et al., 2020; Melini, V. et al., 2021; Katsi, P. et al., 2021).

All of them applied conventional analytical methods based on techniques such as, chromatography or atomic absorption spectroscopy that are tedious, time-consuming, require complex sample pretreatments involving the use of various solvents, long extraction stages, etc., and are destructive. As an alternative to the classical methods used to study the bread quality, some reported studies have developed analytical methods based on faster, non-destructive, and non-invasive techniques, such as, imaging techniques (Amigo, J. et al., 2021; Olakanmi, S.J. et al., 2024; de Almeida Duarte et al., 2022; Verdú, S. et al., 2016). Amigo, J. et al., studied the effect of staling process on white bread crumb using near infrared hyperspectral imaging (NIR-HSI). Olakanmi, S.J. et al. characterised the protein content in nutritionally enriched bread using hyperspectral imaging (HSI) in visible-near-infrared (VNIR) and in short-wave infrared spectral (SWIR) range. De Almeida Duarte, E.S. et al. quantified and authenticated the cassava starch content in wheat flour for bread-making using NIR spectroscopy and digital images. Verdú, S. et al. detected adulterations with different cereal flours in wheat bread using HSI in NIR and SWIR spectral range. All the above studies combined imaging techniques with chemometric tools to obtain relevant chemical information.

Despite the large number of published studies focusing on bread quality, there is no known analytical solution to verify the content of wholemeal flour in marketed bread. The only current way to establish quality control in this context is to carry out on-site inspections at the production plants. Under this scenario, the present study proposes a solution consisting on a new methodology based on HSI techniques.

HSI is a promising analytical platform for quality and safety food assessment, since it is a rapid, non-destructive, non-invasive, and environmentally friendly technique requiring minimal sample preparation (Huang, H. et al., 2014; Saha, D. & Manickavasagan, A., 2021; An, D. et al., 2023). Note that HSI presents the advantages of traditional spectroscopy (results in obtained in a very short time, applied directly on the intact raw samples, and using a green methodology). Commonly, computer vision (so-called machine vision), can provide three-dimensional information for the simultaneous measurement of quality and safety attributes. The representation of a hyperspectral image is achieved through a three-dimensional data structure known as a data cube (or hyperspectral cube), where each pixel in the image is defined by its X and Y positions (spatial coordinates), has an associated value in each spectral band (spectral coordinates), which captures information about the reflected or emitted light in a specific region of the electromagnetic spectrum.

Owing to the large data volume within the data cube, advanced data processing tools inherent to data mining must be applied. Data mining tools enable the reduction of the size of a data set, eliminate noise and interferences resulting from the recorded analytical signal and correct effects such as scattering, baseline drift, etc. (Basantia, N. C. et al., 2018). After their application, a pretreated image which contains the spectral fingerprints characteristic of the test sample is obtained. Once this image is collected, multivariate analytical methods can be applied using tools like principal component analysis (PCA), partial least square discriminant analysis (PLS-DA), support vector machine (SVM), etc. Aligning with this, some authors have proposed the use of these tools to carry out qualitative and quantitative studies from signals obtained by HSI (Sampaio, P.S. et al., 2020; Li, F.L. et al., 2021; Sarkar, S. et al., 2020). For example, Sampaio, P.S. et al., identified different kinds of rice using, firstly, PCA and PLS-DA as a screening analysis, and secondly, used SVM to classify their samples according to the rice variety. Li, F.L. et al., quantified the content of the mycotoxin DON in wheat flour using

PLS. Sarkar, S et al. compared the results obtained from SVM and PLS application to quantify the soluble solids content in kiwi fruit. The last two studies are a clear example of the strategy commonly followed to quantify components through imaging techniques. Until now, the analytical studies focused on detecting and quantifying components in samples through spectral images have been based on the construction of quantification models using multivariate analysis methods. PLS and SVM are the most used. When the relationship between the spectral data and the measured parameters is linear, the best results were obtained by PLS (Rady, A. & Adedeji, A.A., 2020; Wiley, V. & Lucas, T., 2018; Femenias, A. et al., 2020). However, SVM has proven to achieve better results when the relationship is non-linear (Jiang, X. et al., 2022).

Many researchers have developed analytical methods focused on component quantification to assess the quality of different foodstuffs (Liu, H. Y. et al., 2023; Perez, M., et al., 2023; Qin, C. et al., 2022; Candoğan, K. et al., 2021), but, to our knowledge, there are no known methods which use HSI and chemometrics to authenticate the content of wholemeal flour in bread. Thus, the aim of the present study is to develop an analytical method based on HSI in conjunction with chemometric tools to authenticate the content of wholemeal flour in bread, which does not require to identify which chemical compound belongs to which band as other analytical techniques usually do. For this purpose, bread samples were prepared from different wholemeal flour proportions from different cereals, considering the most common composition used in the market. Then, the content of wholemeal flour was determined by imaging with a spectral camera in the visible and near-infrared range in combination with chemometric tools and a proposed *ad-hoc* data analysis method named *quantification based on pixel counting by classification* (QPC).

QPC methodology stemmed from the hypothesis that images captured from bread elaborated exclusively with a single kind of flour (white or wholemeal) contain spectral homogeneous pixels, while mixed bread present a greater spectral heterogeneous. In both cases, bread would be a homogeneous material. However, mixed bread exhibits dispersed particles into the material which arise heterogeneity. These discernible particles, located in certain pixels, could be captured through HSI and quantified using the methodology proposed in this study.

2. Materials and methods

2.1. Bread samples

A total of 159 homemade bread samples were prepared, of which 59 were made entirely with white flour, 52 with wholemeal flour only, and 48 using different proportions of wholemeal and white flours (mixed samples). The proportions in the mixtures included those usually present in marketed mixed wholemeal breads in Spain: 30%, 50% and 70% wholemeal flour. In addition, this study included bread made with 10% and 90% wholemeal flour. Fifteen of the samples (7 only made with white flour and 8 only with wholemeal flour) were prepared at different times and by a different operator to validate the classification models developed in this study. For bread baking, two home bread makers (TAURUS, My Bread. Barcelona, Spain and Cecotec, Bread&Co, Valencia, Spain) were used. The ingredients were water (180 mL), sugar (8 g), salt (3 g), flour (300 g), yeast (7 g) and extra virgin olive oil (22 g). Each bread was made with flour from one or two cereal varieties, including wheat, rye, spelt, and oats, purchased from local grocery shops. The crust of the homemade breads was discarded, and the crumb was dehydrated by drying in an oven (JP Selecta, Barcelona, Spain) at 105 °C for 1 h. Dried breads were ground using a hand blender and vacuum-packed in a plastic bag. All samples were stored under frozen conditions (-20 °C) to prevent deterioration before the measurements.

The samples were placed in Petri dishes of 6 cm diameter and 1.5 cm high, filled to the top, and left until room temperature was reached.

2.2. HSI measurement

HSI images were collected using a Resonon Pika L (Resonon Inc., Integrys, Mississauga, Canada) hyperspectral camera working in reflectance mode. This camera, by default, works covering the spectral range from 384 to 1018 nm with 300 bands. After applying spectral binning and data interpolation, our spectral information ranges from 400 to 1000 nm with a 5 nm interval (121 bands). The size of the sensor is 900 pixels, the focal length is 23 mm, and the capturing distance was 60 cm. The exposure time used was 2.2 ms/line and the framerate of the acquisition was 249 fps. This allowed to capture batches of 8 samples (in a 2 x 4 set up as it can be seen in Fig. 1A), in approximately 4.5 s.

The illumination system consists of a set of 4 stabilized halogen lamps placed at an angle of approximately 45°. Calibration was performed using dark signal (with the lens occluded), and a reference white tile of Zenith Polymer® (SphereOptics GmbH., Herrsching am Ammersee, Germany) of approximately 90% reflectance. Hence, the workflow followed for the capturing and processing of the hyperspectral images was the following: first, the system was focused using a focusing target consisting on thin lines, allowing us to get live sharp images of this target. The exposure time is then set by the use of a reference white tile. This exposure settings are the ones used for all captures (Sample_raw, White and Black). Afterwards the white tile is scanned. Since the tile is spatially uniform, this image (White), is used afterwards as shown in eq. (1) to compensate the non-uniformity of the illumination. Later on, the dark image (Dark), is captured covering the camera lens with a cap, and will be used for subtracting the dark noise from the spectral images. Finally, the samples are captured in batches of 8 samples (Sample_raw) as mentioned before.

All captured images were corrected into reflectance images (Sample_ref), using the known spectral reflectance of the white tile (White_ref) as indicated in equation (1):

$$\text{Sample}_{\text{ref}} = \frac{\text{Sample}_{\text{raw}} - \text{Dark}}{\text{White} - \text{Dark}} \text{White}_{\text{ref}} \quad (1)$$

2.3. Sample data handling

The HSI images were captured over batches of samples. Each batch included 8 samples placed in different Petri dishes, which were arranged in two rows and four columns (2 × 4) on a white platform for spectral scanning. The first sample of each batch was consistently kept in the same position throughout all captures as a quality control. HSI images were stored as a 'band interleaved by line' file (.bil) and converted to MATLAB file format later (.mat). MATLAB Hyperspectral Toolbox was used to visualise captured images (R2019a version, Mathworks Inc., Natick, MA, USA).

Once the image was opened, a region of interest (ROI) for each sample was selected using a data processing MATLAB function developed by the *Color Imaging Lab* of the University of Granada. This process involved clicking on the centre of the image corresponding to each sample and defining a 225 × 225 pixels area. Each pixel contained a spectrum with 121 spectral bands. As a result, each ROI consisted of a 3D data structure (ROI data cube) of 225 × 225 × 121 elements, which is a total of 50,625 spectra (i.e., 6,125,625 reflectance values) per sample. For each ROI data cube, the representative average spectrum of each sample was computed and stored separately.

In order to verify that the imaging conditions remained unchanged throughout the capturing process, a similarity analysis was performed on the spectra of the batch-to-batch control samples. In this regard, the nearness index (NEAR) was calculated between each pair of average spectra (Arroyo-Cerezo, A. et al., 2023). This index measures the Euclidean distance between two vectors, each of which define a spectrum. Equation (2) defines this index for the vectors \mathbf{Y}_A and \mathbf{Y}_B , where d^N is the normalised distance and d_{max} is the maximum distance between points. Nearness index is 0–1 normalised, where values close to 1

indicate a high similarity between spectra, and therefore no changes in the analysis conditions. The conformity limit was established for values surpassing 0.95.

$$\text{NEAR}(\mathbf{Y}_A, \mathbf{Y}_B) = 1 - d^N(\mathbf{Y}_A, \mathbf{Y}_B) = 1 - \frac{d(\mathbf{Y}_A, \mathbf{Y}_B)}{d_{\text{max}}(\mathbf{Y}_A, \mathbf{Y}_B)} = 1 - \sqrt{\frac{\sum (y_{Ai} - y_{Bi})^2}{\sum (y_{Ai} + y_{Bi})^2}} \quad (2)$$

Once the consistency of the quality control samples was ensured, the analysis of the data samples was carried out.

Due to the large volume of data, a double reduction of the ROI data cube was performed: (1) a dimensionality reduction, and (2) a reduction of the number of elements. To achieve this, a reduced sample data matrix was extracted from each ROI data cube using a home-made MATLAB function. This new representative data matrix for each sample consisted of 100 randomly selected pixels and their corresponding spectra, resulting in a 2D data structure of 100 × 121 elements (i.e., 100 unfolded spectra each consisting of 121 reflectance values, with a total of 12,100 values). Additionally, for each sample data matrix, a representative average spectrum was computed (see Fig. 1A).

In all cases, both ROI cube and matrix sample average spectra were previously scaled by performing standard normal variance (SNV) as pre-processing method to correct for both baseline shift and global intensity variations.

2.4. Evaluation of data homogeneity

Two data homogeneity evaluation procedures were carried out before proceeding to build the classification model. The first one was aimed at assessing the representativeness of each 100-pixel sample data matrix in respect to the 50,625-pixel ROI data cube. If the extracted data matrix is consistent with the ROI data cube, the average spectrum obtained from that matrix should show a high similarity to the average spectrum of the starting ROI cube. In addition, if different extractions of random 100 pixels spectra are performed, the average spectra of each of the matrices should all be similar to each other.

The second evaluation was intended to verify the spectral similarity between pixels within the same sample data matrix. If pixels present high similarity, the matrix is spectrally homogeneous, which should be related to the composition of the sample. The images of bread samples made from the same type of flour (100% white or 100% wholemeal) are expected to show high inter-pixel homogeneity, i.e, a high inter-pixel spectral similarity. Conversely, images captured from bread samples produced from a mixture of white and wholemeal flour will contain pixels that are more heterogeneous.

2.4.1. Homogeneity between sample matrices from a same ROI cube

To perform this evaluation, one ROI data cube was randomly chosen for each of the three kinds of bread samples considered in this study (white flour, wholemeal and 50% flour mix). Then, 10 sample data matrices were randomly extracted from each of these ROI cubes as explained in section 2.3. To evaluate the similarity between matrices from the same sample, a NEAR-based similarity analysis was conducted, comparing between the average spectra of each of the 10 sample matrices and the average spectrum of the ROI cube (see Fig. 1B).

2.4.2. Inter-pixel homogeneity within a sample matrix

From each set of 10 sample matrices used in the previous study, one was again randomly chosen to test for inter-pixel homogeneity. Unlike in the previous section, the spectral comparison was performed by running a hierarchical cluster analysis (HCA) deployed in MATLAB PLS_Toolbox on the pre-processed pixel-spectra. In this way, the analysis will identify pixel grouping according to their spectral information. Ward's method was applied as a linkage criterion among groups of pixel spectra and

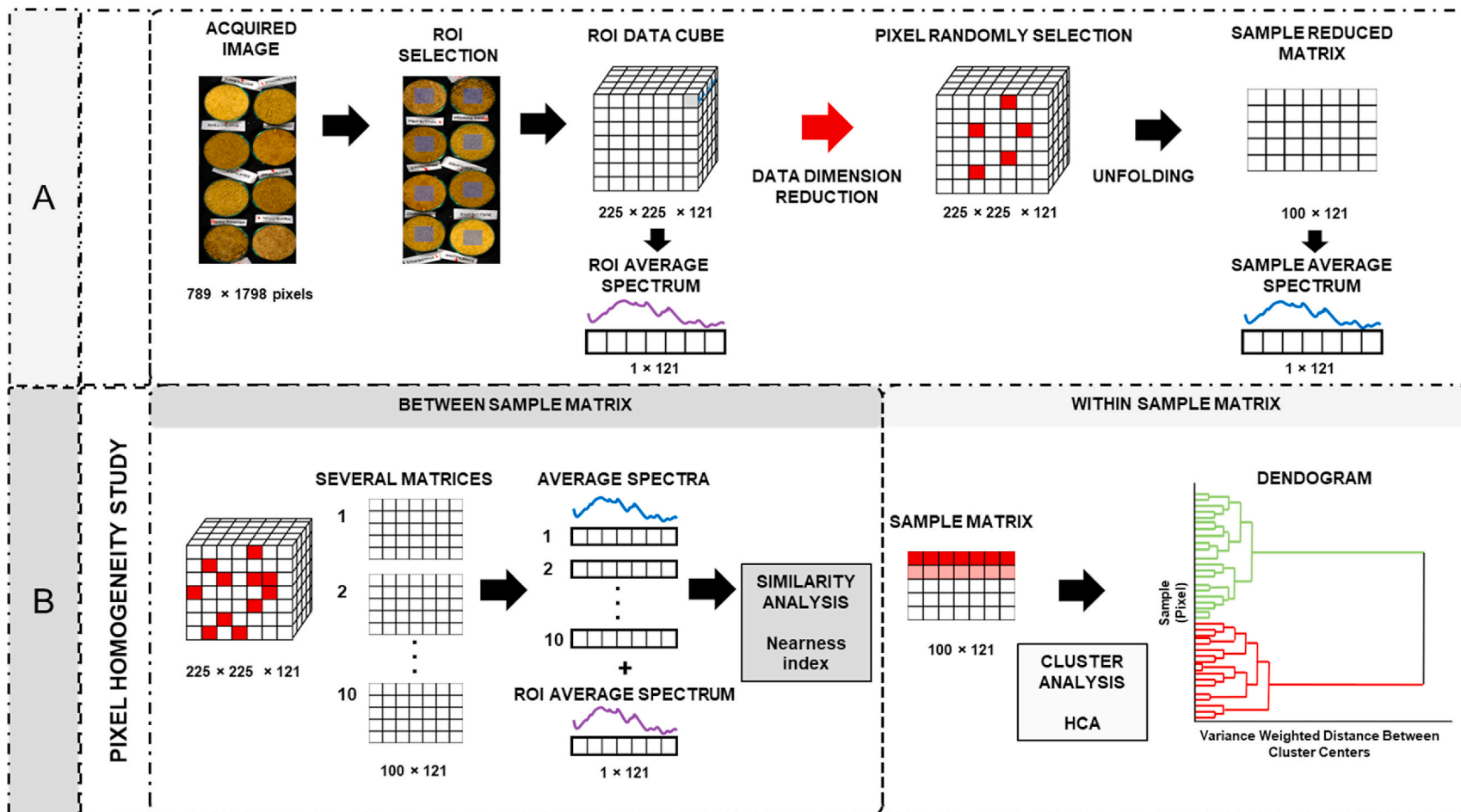


Fig. 1. Flowchart showing both stages performed for (A) sample data handling and (B) homogeneity study.

Manhattan distance was employed as a measure of distance between pairs of spectra. The distance at which the first clustering pair opens, read on a dendrogram, will determine the degree of inter-pixel spectral heterogeneity or homogeneity within the sample matrix image. It is expected that bread samples prepared from the same type of flour will have a significantly smaller distance than bread samples containing mixed flour. If this is indeed the case, this provides a potential method for the quantification of the proportion of each type of flour through identification of the pixels belonging to each of the two clusters. This method (QPC) is described in the next section.

2.5. Quantification based on pixel counting by classification (QPC)

The inter-pixel homogeneity study of a mixed flour sample (section 2.4.) reveals a continuous separation between two main clusters of pixels over a large distance interval (i.e., the length of the distinctive branches of each cluster are significantly larger than those of the following segments). Based on this first finding, a quantification method to estimate the wholemeal flour content in bread samples has been developed. It is based on a preliminary binary classification model that differentiates between the two types of pixels according to their characteristic spectrum. To train this model, two classes are defined using the average spectra obtained from the ROI cubes: (1) the pure wholemeal flour ('Wholemeal' class), and (2) the pure white flour ('White' class). Only the average spectra of the samples obtained with pure flour are used in the training phase.

Once the classifier is trained it is tested on the 100 individual pixel spectra extracted from each mixed sample in our data set. As a result, the spectra will be distributed between the two classes, so that each pixel will be assigned to one of the classes. Just by counting the pixels assigned to the 'Wholemeal' class, an estimate of the proportion of wholemeal flour in the bread is obtained. The classification process is repeated for each sample under analysis. This innovative quantification methodology is proposed and applied for the first time in this paper and has been referred to by the authors as *quantification based on pixel counting by classification* (QPC).

Previously, a non-supervised exploratory analysis was performed in order to screen if the initial hypothesis formulated using the HCA results is valid. The details of the whole process are described in the following subsections.

2.5.1. Screening analysis

Principal component analysis (PCA) and partial least-squares regression (PLS) were firstly applied in order to perform a screening analysis of the 144 sample average spectra, to confirm the results suggested by the HCA method. This screening analysis was aimed at exploring whether the natural grouping by clustering of the sample spectra is caused by the presence - or absence of wholemeal flour.

2.5.2. Classification models for evaluating wholemeal/white bread samples

Two classification methods were applied in this study: partial least square-discriminant analysis (PLS-DA) and support vector machine (SVM). Both methods were used to authenticate the wholemeal flour composition in bread samples, considering only samples made entirely with white or wholemeal flour (excluding mixed samples). For each method (PLS-DA and SVM), a total of 96 sample average spectra were used for building a classification model (52 spectra of white flour bread samples and 44 of wholemeal flour bread samples). The sample set was accordingly divided in two groups: 'Wholemeal' and 'White': 'Wholemeal' set consisted of samples elaborated only from wholemeal flour and 'White' set of samples from white flour. In turn, each sample set was partitioned into two subgroups: a training set, constituting 70% of the total spectra (68 samples), and an external validation set (Validation Set 1) comprising the remaining ones (28 samples). Notice that the validation was conducted under repeatability conditions, i.e., the spectra involved in the model building and validation were captured from bread

samples produced under the same conditions (production process, time, operator, etc.). Once the classification model is built and initially validated, an additional external validation (Validation Set 2) was performed using a new sample set not included in the model development, which consisted of 15 bread samples produced from different batches of flour, on various dates and by a distinct operator. In this way the built model was reliably evaluated under real in-house scenarios with varying production conditions. Detailed information on the number and type of samples used for the validation of the model is shown in Table 1. Additionally, a scheme of the classification model development was included in supplementary material (see FS2).

The CADEX algorithm, i.e., Kennard-Stone's method, was employed to select the pixel-spectra of the validation set (Kennard, R. W., & Stone, L. A. 1969). For the SVM analysis, a radial basis function (RBF) was selected as a kernel function. The main quality metrics of each classification model (sensitivity, specificity, precision and accuracy) are then assessed.

2.5.3. Quantification of the wholemeal flour percentage

According to the values of quality metrics, the best classification model was selected, and then the QPC methodology was applied to estimate the percentage of wholemeal flour in each flour mix bread sample. Each pixel-spectrum was classified either as 'Wholemeal' or 'White'. The number of pixel-spectra classified as 'Wholemeal' directly represents the percentage of wholemeal flour searched. This process was consecutively performed for each mixed flour sample. A linear regression was used to relate QPC percentage values vs. nominal percentage values of wholemeal. In addition the assessment of the performance of the QPC method was based on estimating the main quantification metrics calculated on the validation set, i.e., the coefficient of determination (R^2), the root mean square error of validation (RMSEV), the mean absolute error of validation (MAEV), the median absolute error of validation (MdAEV), and standard deviation of validation residuals (SDV), as recommended by ASTM E2617 standard (ASTM E2617-17, 2017).

3. Results and discussions

3.1. Evaluation of pixels homogeneity

Two pixels homogeneity evaluation methods were used in the present study. The results and findings are detailed below.

3.1.1. Homogeneity between sample matrices from a same ROI cube

NEAR similarity index was calculated to assess the representativeness of each 100-pixel sample data matrix with respect to the ROI data cube. This estimation was performed taking one sample for each kind of bread made with different flour (white flour, wholemeal and 50% flour mix) as a representative example, using 10 average spectra derived from 10 different data matrices within each sample, and its corresponding ROI average spectrum. Consequently, 11 spectra per sample were compared.

Table 1

Information about the type and number of bread samples used for the external validation of PLS-DA and SVM.

External validation set	Classification method	Number and type of samples
1	PLS-DA	10 (100% white flour)
		18 (100% wholemeal flour)
	SVM	10 (100% white flour)
		18 (100% wholemeal flour)
2	PLS-DA	7 (100% white flour)
		8 (100% wholemeal flour)
	SVM	7 (100% white flour)
		8 (100% wholemeal flour)

PLS-DA: partial least squares – discriminant analysis; SVM: support vector machine.

The nearness index (NEAR) is based on the proximity of two data vectors, i.e., spectra, in space so that the closer they are, the greater the similarity is. Moreover, it is normalised to range between 0 and 1, with 0 meaning complete dissimilarity and 1 totally identical. As detailed in Table 2, the NEAR average value resulting from comparing the 11 spectra of each sample varied between 0.96 and 0.94. These values underscore the high degree of similarity between average spectra derived from different sample data matrix. Consequently, any 100-pixel data matrix extracted from the ROI data cube could be representative of it. Thus, the reduction of data dimensionality and the reduction of the number of ROI data cube elements are viable, facilitating data management in the study.

3.1.2. Inter-pixel homogeneity within a sample matrix

In order to evaluate the spectral similarity between sample pixels, three of the sample data matrices used in the previous study, one per kind of bread sample (white flour, wholemeal and 50% flour mix), were assessed using HCA. The results of HCA were presented in a dendrogram in which the relationships between pixel spectra are shown.

The clustering pixels from each type of sample are shown in Fig. 2. Notably, samples made exclusively with one kind of flour (Fig. 2A and B) present a dendrogram structure that is more compact with shorter branches. Additionally, the distance measured between the first pixel groupings was shorter compared with flour mix sample (Fig. 2C). These results indicate homogeneous behaviour among pixels from samples made with the same type of flour. In other words, pixels belonging to 100% white or wholemeal flour samples share a high degree of spectral similarity, reflecting a more uniform composition. Therefore, the average spectrum in such cases would accurately capture the representative spectral characteristics of the entire sample. Conversely, the sample made with flour mix exhibits greater variability among pixels, leading more dispersed dendrogram structure and larger distances between the first groupings. In this scenario, the average spectrum might not contain all the spectral attributes of the entire sample.

In short, HCA analysis provided compelling evidence confirming that single-type flour samples exhibit higher spectral homogeneity than mixtures.

3.2. Screening analysis

PCA and PLS were applied as multivariate analysis methods to identify behavioural patterns among samples, assessing their correlation with the presence or absence of wholemeal flour in bread composition.

3.2.1. Principal component analysis

PCA was performed using a dataset consisting of 144 average spectra derived from bread samples, represented by 121 variables (i.e., wavelengths). PC1 and PC2 accounted for 94.31% and 3.78% of the total variance (97.98%). The scores plot of PC1 and PC2 represents the most significant variability among the samples (Fig. 3A). Red rhombuses represent the average spectra of bread samples exclusively made with white flour, green squares samples exclusively made with wholemeal and blue triangle samples made with different proportions of both flours. As can be seen from the plot, most of the white bread samples tended to localize toward negative values of PC1. In contrast, all the wholemeal samples were located in positive values. Samples made with

Table 2
Values of NEAR similarity index comparing 10 average spectra from 10 sample data matrix and the ROI average spectrum.

Experience Run	Sample composition	Min value	Max value	Average value
1	100% white flour	0.888	0.997	0.962
2	100% wholemeal flour	0.879	0.997	0.946
3	50% flour mixed	0.885	0.999	0.968

different proportions of both flours were located between positive and negative PC1 values, between the two groups (White flour and Wholemeal flour). One important aspect to highlight is that mixed samples do not form a separated group suggesting that their differences are related to the proportion of white and wholemeal flours, and it could explain their tendency to locate close to one or other sample groups. Thus, PLS was performed as a complementary screening analysis.

3.2.2. Partial least squares

To verify whether the grouping tendency among bread samples is associated with the type and amount of flour used in their production, a PLS analysis was performed using the average spectrum of the samples involved in the previous study. Samples were labelled indicating their percentage of wholemeal flour content, with label 0 being the samples made exclusively from white flour and 100 samples made only from wholemeal flour. Fig. 3B shows the scores plot of LV1 versus LV2, where LV1 explained 94.24% of the total variance between the samples and LV2 explained 3.75%. The samples with a nil percentage of wholemeal flour content tended to present the most negative values along LV1. Moreover, when the percentage of wholemeal flour increases, the samples tend to separate gradually from negative to positive values along LV1. This gradual separation is particularly noticeable in samples with a percentage of wholemeal flour less than 50%. After these results, it was concluded that the best option was to build a classification model with the aim of separating samples made with any proportion of wholemeal flour from samples made only with white flour.

3.3. Classification models for evaluating wholemeal/white bread samples

Two multivariate analysis methods, PLS-DA and SVM, were used to build a classification model to discriminate between bread samples only made with white flour and bread samples only made with wholemeal flour. Accordingly, two classes were defined for the classification models: Wholemeal (target class) and White (alternative class). A total of 68 bread samples included in any of these two classes were selected to build the training set, and 28 samples were used for model external validation set 1, and 15 samples were employed for external validation set 2.

3.3.1. Partial least squares discriminant analysis

PLS-DA model was developed with 3 latent variables (LVs), explaining 95,83% and 71,51% of the accumulative variances over the x-variable and y-variable blocks. Then, the model was validated considering two different external validation sets (see Table 1) whose classification plots and classification results in terms of quality parameters are shown in Fig. 4 and Table 3, respectively. The purple line shown in this figure is the threshold established to separate between "White" and "Wholemeal" samples. Moreover, the overall quality metrics representatives of the classification were estimated from the pooled average of the corresponding metrics regarding the results and the number of samples from the two classes. Resulting in 86% sensitivity, 81% specificity, 86% accuracy and 100% precision. Note that, the external validation step was not performed sequentially, i.e. once the external validation was carried out on the first set, this set was used to feed back the model and then external validation was carried out again on external validation set 2.

In order to locate the region of the spectral fingerprint which contains characteristic information to discriminate between "White" and "Wholemeal" classes, the LV1 PLS-DA scores and loading plots were evaluated. Fig. S1A (supplementary material) reveals that the most of "White" samples have negative scores on LV1 axis while, "Wholemeal" samples present positive scores on this axis. Accordingly, LV1 loading plot was evaluated (Fig. 1SB). The 66–121 variable interval correspond to LV1 positive loadings which could be considered as the discriminative region being characteristic of "Wholemeal" class while the 1–65 variable interval is characteristic of "White" class.

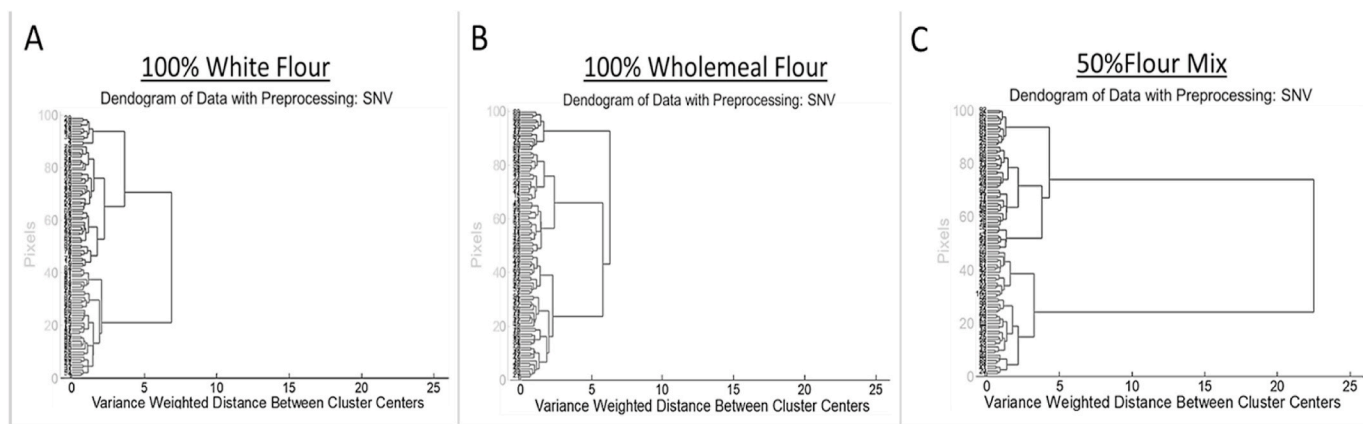


Fig. 2. Dendrogram of bread samples: (A) white flour bread sample; (B) wholemeal bread sample; (C) Flour mixed bread sample.

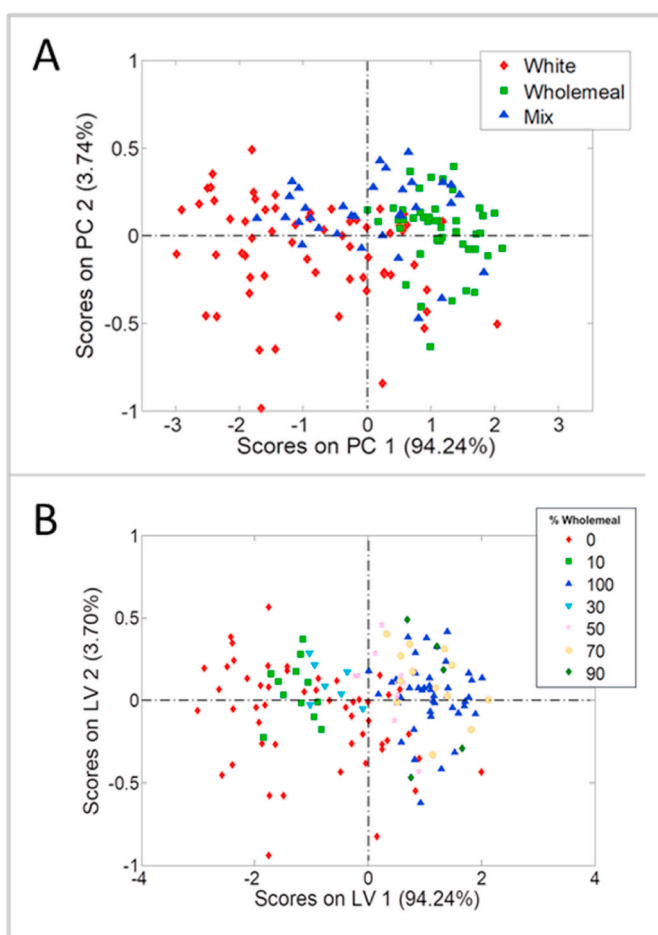


Fig. 3. PCA and PLS cores plot using the average spectra of 144 bread samples labelled as White, Wholemeal or Mix, according to their flour composition: (A) PCA scores plot of PC1 versus PC2; (B) PLS scores plot of LV1 versus LV2.

Likewise, the variable importance in projection (VIP) scores plot of the PLS-DA model was examined (see Fig. 5A). VIP scores is a metric for assessing the significance of each variable (i.e., wavelengths) within the classification model. The variables that present high VIP values are particularly influential in the discrimination of Wholemeal and White classes. In this case, VIP plot reveals two regions where the values are higher than the rest: one centered around variable 40 and another region around variable 120 (see Fig. 5A). To show the wavelengths that correspond to these variables, two raw average spectra from white and

wholemeal samples are compared (see Fig. 5B). The discriminant spectral regions between the two classes were highlighted in purple and correspond to 600 and 1000 nm. The plotted spectrum of wholemeal sample exhibits a lower reflectance compared to white sample at 600 nm, while the opposite is observed at 1000 nm. Thus, these spectral regions could be considered as discriminant regions between Wholemeal and White classes. It suggests the possibility of working with a multi-spectral camera in these two spectral regions, instead of hyperspectral camera, thereby cutting down on analysis costs.

Differences around the 600 nm wavelength band are likely due to the colour differences of white and wholemeal samples; being that the higher wholemeal flour content a sample has, the lower the measured reflectance. Furthermore, spectral band analysis could be made in the NIR region of the analysed spectra. More specifically, around the 900–1000 nm wavelength range, a clear distinction may be made between the wholemeal and white spectra, which correspond to the second overtone region of –OH bonds (Xiaobo, Z. et al., 2010). This could be due to the difference between the composition of wholemeal and white flour. While white flour only contains the endosperm (which has high starchy carbohydrate content), wholemeal flour preserves all the cereal components. These other components contain a lower amount of carbohydrates and higher protein content than endosperm (Harris, P.J., et al., 1993; Khalid, A. et al., 2023). Therefore, high starchy carbohydrate content could likely be the reason that explains the lower reflectance values measured in the 900–1000 nm range.

3.3.2. Support vector machine

Using the same training and validation sets as PLS-DA, SVM was employed as nonlinear computational learning method to build a bread classification model.

For this purpose, the methodology outlined in the previous section was followed. Firstly, the model was validated using the validation set 1 consisting of 28 samples. Next, the model was fed back using this validation set 1, and then it was revalidated with the 15 bread samples prepared at another time by another analyst (validation set 2). The classification plots as well as the quality parameters are shown in Fig. 6 and Table 3, respectively. The purple line shown in this figure is the threshold established to separate between "White" and "Wholemeal" samples. Unlike PLS-DA, SVM yielded better results in discriminating between bread made with 100% whole wheat flour and those that were not. These results led to the decision to apply SVM as classifier instead of PLS-DA in the subsequent stage of the study, which focused on quantifying the amount of whole wheat flour.

3.4. Authentication of wholemeal flour content in bread samples

The quantification of wholemeal flour content was carried out

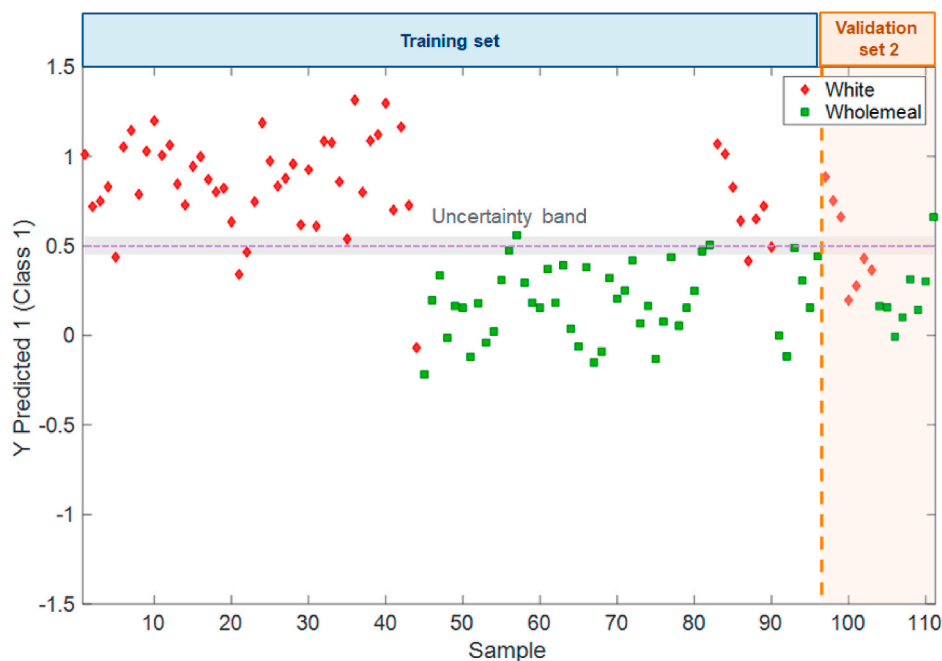


Fig. 4. Classification plot of the validation set bread samples classification performed by PLS-DA considering two classes: Wholemeal and White. Note: The purple line indicates the discrimination threshold established to separate between "White" and "Wholemeal" samples; Uncertainty band (grey) is the region of inconclusive classification.

Table 3
Summary of classification performance metrics from PLS-DA and SVM models.

External validation set	Classification method	Quality Performance metric	Wholemeal class	Pooled ^a
1	PLS-DA	Specificity	0.94	0.86
		Sensitivity	0.73	0.81
		Precision	1.00	1.00
	SVM	Accuracy	0.86	0.86
		Specificity	0.94	0.89
		Sensitivity	0.82	0.87
2	PLS-DA	Precision	0.89	0.89
		Accuracy	0.89	0.89
		Specificity	0.88	0.67
	SVM	Sensitivity	0.43	0.64
		Precision	0.64	0.81
		Accuracy	0.67	0.67
SVM	Specificity	0.88	0.80	
	Sensitivity	0.71	0.79	
	Precision	0.78	0.80	
	Accuracy	0.80	0.80	

^a Pooled: weighted average of quality metrics for the classification process with two input-classes: Wholemeal and White.

applying the QPC methodology explained in detail in section 2.5. In this regard, after evaluating that SVM yielded better results as a classification method (3.3 section), it was selected as the classifier and used to determine the percentage of wholemeal flour analysing one-by-one 48 bread samples made with flour mix.

Fig. 7 illustrates an example of QPC application to a bread sample made with a 70% of wholemeal flour. SVM model was applied to classify the sample pixels as Wholemeal or White. In this case, a total of 76 pixels were classified as Wholemeal. This would involve that the sample percentage of wholemeal flour is 76%. The results for the 48 bread samples (see Table S1 of the supplementary material) were evaluated following the same methodology yielding an R^2 of 0.94, indicating a high degree of agreement between predicted and nominal values, coupled with relatively low RMSEV of 7.77 and MAEV of 7.00. Furthermore, a MdAEV of

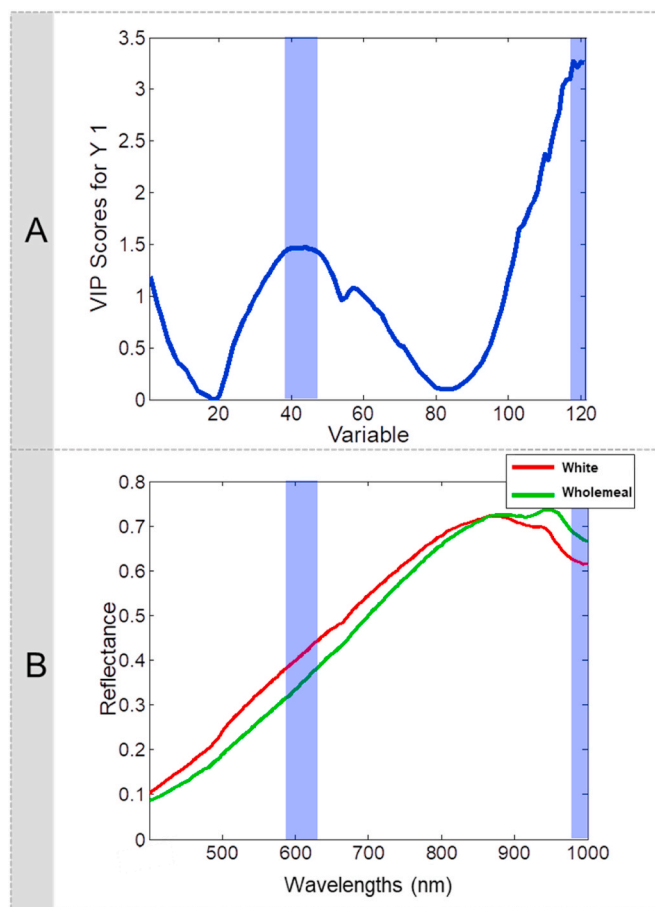


Fig. 5. Specified discriminant windows concerning the classification between Wholemeal and White samples, located over the VIP plot (A), and the spectra (B).

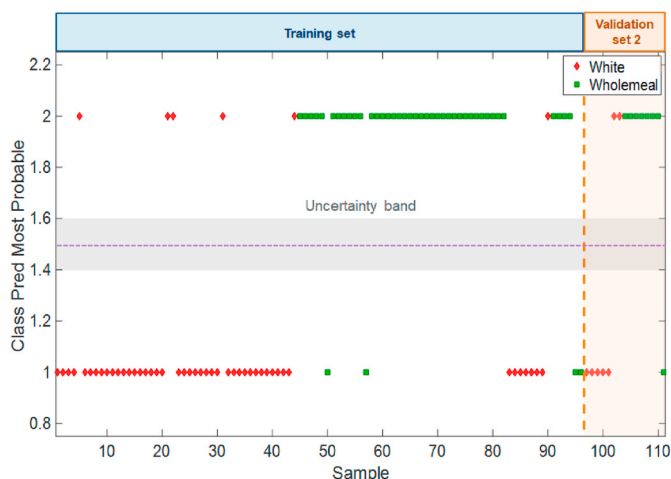


Fig. 6. Classification plot of the validation set bread samples classification performed by SVM considering two classes: Wholemeal and White. Note: The purple line indicates the discrimination threshold established to separate between "White" and "Wholemeal" samples; Uncertainty band (grey) is the region of inconclusive classification.

6.48 and SDV of 6.94 were obtained (values expressed in g of wholemeal flour/100 g of total flour in the bread dough). Note that, the last four quantification metrics are given in g wholemeal flour/100 g flour.

The prediction results which exhibited the greatest deviation from the nominal value were observed in samples containing blends of various cereal flours, particularly those incorporating white spelt or white oats. This fact can be attributed to the colour similarity of these flours with other kinds of wholemeal flours. Nevertheless, the results exhibited a maximum deviation of 8 units from the estimated value. This underlines the model's ability to predict wholemeal flour content in breads, irrespective of the kind of the cereal flours used.

4. Conclusions and future perspectives

A new and innovative methodology for wholemeal bread authentication based on hyperspectral imaging (HSI) named QPC was developed in this study. This was able to predict the wholemeal flour content in

flour mixed bread with a maximum deviation of 8 g wholemeal flour/100 g total flour from the estimated value, irrespective of the kind of the cereal flours used in its production. Considering the common prevalence of 30%, 50% and 70% wholemeal flour percentages in marketed breads, this method exhibits considerable potential for addressing the current lack of official methods to authenticate the wholemeal composition in breads. Furthermore, a classification model trained with average spectra was also developed to assess whether the bread is produced with white flour or whole wheat flour, achieving results above 80% accuracy, sensitivity, and specificity.

In essence, the methodology presented would represent the analytical solution to the current gap in the authentication control of this highly consumed food product from an environmentally friendly perspective.

Funding

This work was financially supported by the Grant (RYC2021-031993-I) funded by MCIN/AEI/501100011033 and "European Union NextGeneration EU/PRTR".

CRediT authorship contribution statement

Miriam Medina-García: Writing – original draft, Validation, Software, Methodology, Investigation, Formal analysis, Conceptualization. **Esteban A. Roca-Nasser:** Writing – original draft, Methodology. **Miguel A. Martínez-Domingo:** Writing – review & editing, Supervision, Software, Methodology, Formal analysis. **Eva M Valero:** Writing – review & editing, Visualization, Formal analysis. **Alejandra Arroyo-Cerezo:** Validation, Software, Formal analysis. **Luis Cuadros-Rodríguez:** Writing – review & editing, Validation, Methodology, Investigation, Conceptualization. **Ana M. Jiménez-Carvelo:** Writing – review & editing, Supervision, Resources, Project administration, Methodology, Funding acquisition, Data curation, Conceptualization.

Declaration of competing interest

The authors declare that they have no known competing financial interests or personal relationships that could have appeared to influence the work reported in this paper.

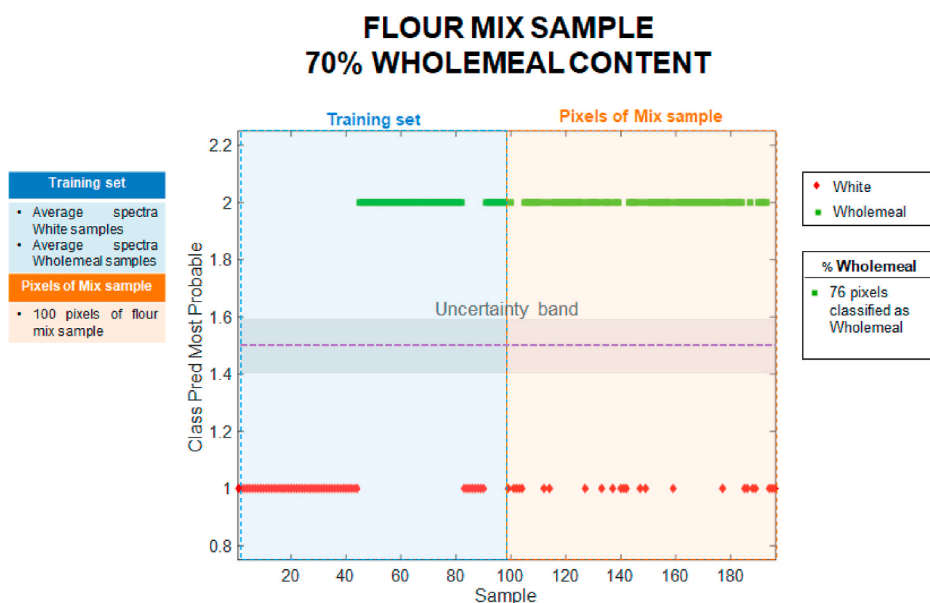


Fig. 7. Example QPC methodology applied to quantify the wholemeal content in a flour mix bread. Note: The purple line indicates the discrimination threshold established to separate between "White" and "Wholemeal" samples; Uncertainty band (grey) is the region of inconclusive classification.

Data availability

Data will be made available on request.

Acknowledgements

AMJC acknowledges the Grant (RYC2021-031993-I) funded by MCIN/AEI/501100011033 and "European Union NextGeneration EU/PRTR". AAC gratefully acknowledges the Spanish Ministry of Universities for a pre-doctoral fellowship FPU (FPU20/04711, Formación del Profesorado Universitario). Funding for open access charge: Universidad de Granada / CBUA.

Appendix A. Supplementary data

Supplementary data to this article can be found online at <https://doi.org/10.1016/j.foodcont.2024.110715>.

References

- Alnaeim, T., Kark, J., & Massri, M. (2014). Chemical composition and energy values of different kinds of bread, biscuit and cereals which cast up by different methods. *Assiut Veterinary Medical Journal*, *60*, 14–22. <https://doi.org/10.21608/avmj.2014.171028>
- Amigo, J. M., Del Olmo, A., Engelsen, M. M., Lundkvist, H., & Engelsen, S. B. (2021). Staling of white wheat bread crumb and effect of maltogenic α -amylases. Part 3: Spatial evolution of bread staling with time by near infrared hyperspectral imaging. *Food Chemistry*, *353*, Article 129478. <https://doi.org/10.1016/j.foodchem.2021.129478>
- An, D., Zhang, L., Liu, Z., Liu, J., & Wei, Y. (2023). Advances in infrared spectroscopy and hyperspectral imaging combined with artificial intelligence for the detection of cereals quality. *Critical Reviews in Food Science and Nutrition*, *63*, 9766–9796. <https://doi.org/10.1080/10408398.2022.2066062>
- Arroyo-Cerezo, A., Medina-García, M., Cuadros-Rodríguez, L., Rutledge, D. N., & Jiménez-Carvelo, A. M. (2023). Chemometric enhancement for blind signal resolution from non-invasive spatially offset Raman spectra. *Chemometrics and Intelligent Laboratory Systems*, *243*. <https://doi.org/10.1016/j.chemolab.2023.105027>. Article 105027.
- ASTM E2617-17. (2017). *Standard practice for validation of empirically derived multivariate calibrations*. ASTM International.
- Hyperspectral imaging analysis and applications for food quality. In Basantia, N. C., Nollet, L. M., & Kamruzzaman, M. (Eds.), *Data extraction and treatment*, (pp. 45–56). (2018) (pp. 45–56). CRC Press. <https://doi.org/10.1201/9781315209203>.
- Candogan, K., Altuntas, E. G., & İğci, N. (2021). Authentication and quality assessment of meat products by fourier-transform infrared (FTIR) spectroscopy. *Food Engineering Reviews*, *13*, 66–91. <https://link.springer.com/article/10.1007/s12393-020-09251-y>.
- Carocho, M., Morales, P., Ciudad-Mulero, M., Fernandez-Ruiz, V., Ferreira, E., Heleno, S., et al. (2020). Comparison of different bread types: Chemical and physical parameters. *Food Chemistry*, *310*. <https://doi.org/10.1016/j.foodchem.2019.125954>. Article 125954.
- de Almeida Duarte, E. S., de Almeida, V. E., da Costa, G. B., de Araújo, M. C. U., Vêras, G., Diniz, P. H. G. D., et al. (2022). Feasibility study on quantification and authentication of the cassava starch content in wheat flour for bread-making using NIR spectroscopy and digital images. *Food Chemistry*, *368*, Article 130843. <https://doi.org/10.1016/j.foodchem.2021.130843>
- De Angelis, M., Minervini, F., Siragusa, S., Rizzello, C. G., & Gobetti, M. (2019). Wholemeal wheat flours drive the microbiome and functional features of wheat sourdoughs. *International Journal of Food Microbiology*, *302*, 35–46. <https://doi.org/10.1016/j.ijfoodmicro.2018.08.009>
- Edwards, W. P. (2007). The science of bakery products. In W. P. Edwards (Ed.), *Introduction* (pp. 1–10). RSC. <https://doi.org/10.1039/9781847557797>.
- Femenias, A., Gatiús, F., Ramos, A. J., Sanchis, V., & Marín, S. (2020). Standardisation of near infrared hyperspectral imaging for quantification and classification of DON contaminated wheat samples. *Food Control*, *111*. <https://doi.org/10.1016/j.foodcont.2019.107074>. Article 107074.
- Gobierno de España. (2019). Boletín Oficial del Estado (BOE). *Real Decreto 308/2019, de 26 de abril, por el que se aprueba la norma de calidad para el pan*, 113 pp. 50168–50175.
- Government of UK (2022). Department for Environment, Food & Rural Affairs. *Food Standards: Labelling and Composition*. <https://www.legislation.gov.uk/uksi/1998/141>. (Accessed 10 January 2024).
- Harris, P. J., & Ferguson, L. R. (1993). Dietary fibre: Its composition and role in protection against colorectal cancer. *Mutation Research: Fundamental and Molecular Mechanisms of Mutagenesis*, *290*(1), 97–110. [https://doi.org/10.1016/0027-5107\(93\)90037-G](https://doi.org/10.1016/0027-5107(93)90037-G)
- Health Promotion Knowledge Gateway. (2022). Whole grain. Knowledge for policy. Retrieved from <https://knowledge4policy.ec.europa.eu/health-promotion-knowledge-gateway/whole-grain.en>. (Accessed 10 January 2024).
- Huang, H., Liu, L., & Ngadi, M. O. (2014). Recent developments in hyperspectral imaging for assessment of food quality and safety. *Sensors*, *14*, 7248–7276. <https://doi.org/10.3390/s140407248>
- Jiang, X., Tian, J., Huang, H., Hu, X., Han, L., Huang, D., et al. (2022). Nondestructive visualization and quantification of total acid and reducing sugar contents in fermented grains by combining spectral and color data through hyperspectral imaging. *Food Chemistry*, *386*. <https://doi.org/10.1016/j.foodchem.2022.132779>. Article 132779.
- Katsi, P., Kosma, I. S., Michailidou, S., Argiriou, A., Badeka, A. V., & Kontomina, M. G. (2021). Characterization of artisanal spontaneous sourdough wheat bread from Central Greece: Evaluation of physico-chemical, microbiological, and sensory properties in relation to conventional yeast leavened wheat bread. *Foods*, *10*, Article 635. <https://doi.org/10.3390/foods10030635>
- Kennard, R. W., & Stone, L. A. (1969). Computer aided design of experiments. *Technometrics*, *11*, 137–148. <https://doi.org/10.2307/1266770>
- Khalid, A., Hameed, A., & Tahir, M. F. (2023). Wheat quality: A review on chemical composition, nutritional attributes, grain anatomy, types, classification, and function of seed storage proteins in bread making quality. *Frontiers in Nutrition*, *10*, Article 1053196. <https://doi.org/10.3389/fnut.2023.1053196>
- Li, F. L., Xie, J., Wang, S., Wang, Y., & Xu, C. H. (2021). Direct qualitative and quantitative determination methodology for massive screening of DON in wheat flour based on multi-molecular infrared spectroscopy (MM-IR) with 2T-2DCOS. *Talanta*, *234*, Article 122653. <https://doi.org/10.1016/j.talanta.2021.122653>
- Liu, H. Y., Wadood, S. A., Xia, Y., Liu, Y., Guo, H., Guo, B. L., et al. (2023). Wheat authentication : an overview on different techniques and chemometric methods. *Critical Reviews in Food Science and Nutrition*, *63*, 33–56. <https://doi.org/10.1080/10408398.2021.1942783>
- Ma, S., Wang, Z., Guo, X., Wang, F., Huang, J., Sun, B., et al. (2021). Sourdough improves the quality of whole-wheat flour products: Mechanisms and challenges a review. *Food Chemistry*, *360*, Article 130038. <https://doi.org/10.1016/j.foodchem.2021.130038>
- Melini, V., Melini, F., & Acquistucci, R. (2021). Nutritional characterization of an Italian traditional bread from ancient grains: the case study of the durum wheat bread "Pane di Monreale". *European Food Research and Technology*, *247*, 193–200. <https://doi.org/10.1007/s00217-020-03617-6>
- Nashat, S., & Abdullah, M. Z. (2016). In D. W. Sun (Ed.) (2nd ed., *Quality evaluation of bakery products* Computer vision technology for food quality evaluation (pp. 525–589). Academic Press. <https://doi.org/10.1016/B978-0-12-802232-0.00021-9>.
- Olakanmi, S. J., Jayas, D. S., Paliwal, J., Chaudhry, M. M. A., & Findlay, C. R. J. (2024). Quality characterization of fava bean-fortified bread using hyperspectral imaging. *Foods*, *13*, 231. <https://doi.org/10.3390/foods13020231>
- Pérez, M., Domínguez-López, I., López-Yerena, A., & Vallverdú Queralt, A. (2023). Current strategies to guarantee the authenticity of coffee. *Critical Reviews in Food Science and Nutrition*, *63*, 539–554. <https://doi.org/10.1080/10408398.2021.1951651>
- Pico, J., Gómez, M., Bernal, J., & Bernal, J. L. (2016). Analytical methods for volatile compounds in wheat bread. *Journal of Chromatography A*, *1428*, 55–71. <https://doi.org/10.1016/j.chroma.2015.09.045>
- Qin, C., Liu, L., Wang, Y., Leng, T., Zhu, M., Gan, B., et al. (2022). Advancement of omics techniques for chemical profile analysis and authentication of milk. *Trends in Food Science & Technology*, *127*, 114–128. <https://doi.org/10.1016/j.tifs.2022.06.001>
- Rady, A., & Adedeji, A. A. (2020). Application of hyperspectral imaging and machine learning methods to detect and quantify adulterants in minced meats. *Food Analytical Methods*, *13*, 970–981. <https://doi.org/10.1007/s12161-020-01719-1>
- Riyanto, R. A., & Caraka, R. E. (2018). Comparative studies on the salt content of white bread and wholemeal bread. In *Journal of physics: Conference series* (Vol. 1025), Article 012116. <https://doi.org/10.1088/1742-6596/1025/1/012116>
- Saha, D., & Manickavasagan, A. (2021). Machine learning techniques for analysis of hyperspectral images to determine quality of food products: A review. *Current Research in Food Science*, *4*, 28–44. <https://doi.org/10.1016/j.crf.2021.01.002>
- Sampaio, P. S., Castanho, A., Almeida, A. S., Oliveira, J., & Brites, C. (2020). Identification of rice flour types with near-infrared spectroscopy associated with PLS-DA and SVM methods. *European Food Research and Technology*, *246*, 527–537. <https://doi.org/10.1007/s00217-019-03419-5>
- Sarkar, S., Basak, J. K., Moon, B. E., & Kim, H. T. (2020). A comparative study of PLSR and SVM-R with various preprocessing techniques for the quantitative determination of soluble solids content of hardy kiwi fruit by a portable vis/NIR spectrometer. *Foods*, *9*. <https://doi.org/10.3390/foods9081078>. Article 1078.
- Verdú, S., Vázquez, F., Grau, R., Ivorra, E., Sánchez, A. J., & Barat, J. M. (2016). Detection of adulterations with different grains in wheat products based on the hyperspectral image technique: The specific cases of flour and bread. *Food Control*, *62*, 373–380. <https://doi.org/10.1016/j.foodcont.2015.11.002>
- Wiley, V., & Lucas, T. (2018). Computer vision and image processing: A paper review. *International of Artificial Intelligence Research*, *2*, 29–36. <https://doi.org/10.29099/ijair.v2i1.42>
- Xiaobo, Z., Jiewen, Z., Povey, M. J., Holmes, M., & Hanpin, M. (2010). Variables selection methods in near-infrared spectroscopy. *Analytica Chimica Acta*, *667*(1–2), 14–32. <https://doi.org/10.1016/j.aca.2010.03.048>
- Yu, L., Nanguet, A. L., & Beta, T. (2013). Comparison of antioxidant properties of refined and whole wheat flour and bread. *Antioxidants*, *2*, 370–383. <https://doi.org/10.3390/antiox2040370>